Full-Scale CFD Simulation of Gypsum Plasterboard Wall Assemblies Exposed to Fire: Effects of Gypsum Dehydration

Full-Scale CFD Simulation of Gypsum Plasterboard Wall Assemblies Exposed to Fire: Effects of Gypsum Dehydration

Dionysios I. Kolaitis; Eleni K. Asimakopoulou; Maria A. Founti*

Laboratory of Heterogeneous Mixtures and Combustion Systems, Thermal Engineering Section,
School of Mechanical Engineering, National Technical University of Athens
9, Heroon Polytechniou St., Polytechnioupoli Zografou, Athens 15780, Greece.
**e-mail: dkol@central.ntua.gr, Tel.: +30-210-7724002, Fax: +30-210-7723527*

ABSTRACT

Gypsum "dehydration" phenomena, occurring when gypsum plasterboard wall assemblies are exposed to a high temperature environment, result in water vapour production and subsequent dispersion in the fire compartment; however, these phenomena are commonly neglected in relevant Computational Fluid Dynamics (CFD) simulations. In order to investigate the impact of gypsum dehydration in full-scale CFD simulations of gypsum plasterboard wall assemblies, the FDS code is used to simulate a two-storey residential building, exposed to a typical domestic fire scenario. A structural steel frame is used in the investigated building, combined with gypsum plasterboard wall assemblies. The effects of gypsum dehydration are taken into account by using a dedicated solid reaction kinetics model; the obtained predictions are compared to a benchmark test case where no such phenomena are modelled. The performed simulations clearly indicate that the explicit simulation of gypsum dehydration phenomena has a prominent effect on CFD predictions; the developed solid reaction kinetics model allows, for the first time, the CFD simulation of gypsum dehydration induced water vapour production and dispersion in the fire compartment.

1 INTRODUCTION

Fire safety regulations have a major impact on the overall design of buildings with regard to layout, aesthetics, function and cost. Historically, fire protection systems in buildings have been commonly regulated using "prescriptive-based" codes and standards; however, prescriptive codes have become complex, exhibiting small or no flexibility for innovative solutions and cost-effective designs. As a result, there is a growing trend worldwide, to implement modern "performance-based" codes, which offer a range of advantages over the prescriptive-based approach. The implementation of performance-based codes requires the utilization of advanced computational tools, capable of describing, in sufficient detail, the large number of physical and chemical phenomena observed in a compartment fire, e.g. fire initiation, spreading and suppression, combustion chemical kinetics, toxicity of combustion products, turbulent flow of gaseous products and smoke, conductive, convective and radiative heat transfer to the structure [1]. Computational Fluid Dynamics (CFD) codes represent the

most advanced computational tools available today and are increasingly used in a wide field of applications related to building fire safety.

Gypsum Plasterboards (GP) are widely used as an aesthetically pleasing, easily applied and mechanically enduring cladding material for walls, floors and ceilings, offering significant fire protection and thermal insulation advantages. When gypsum is subjected to a high temperature environment, water molecules bound in its crystal lattice are released and transferred through its mass; this Gypsum Dehydration (GD) process is highly endothermic, thus enhancing the fire resistance characteristics of the overall structure [2]. Despite the widespread utilization of GP wall assemblies in a large variety of buildings, the interacting physical and chemical phenomena characterizing the GD process are commonly neglected in current CFD simulation studies, thus adversely affecting the quality of the obtained predictions. The present study aims to investigate the impact of GD modelling in the CFD predictions of GP wall assemblies exposed to fire. In this frame, GD phenomena are taken into account by implementing a dedicated solid reaction kinetics numerical model. The macro-scale effects of GD are evaluated by utilizing the developed model, as well as an alternative modelling approach that neglects GD phenomena, in a full-scale CFD simulation of a multi-compartment two-storey residential building exposed to a typical domestic fire.

2 NUMERICAL SIMULATION OF COMPARTMENT FIRES

Despite the important advances made in the area of fire safety science over the last decades, accurate mathematical modelling of compartment fires still poses a significant challenge, since it involves a broad range of interacting physical and chemical phenomena. In addition, the geometrical layout of the compartment significantly affects the characteristics of the developing flow- and thermal-fields (e.g. spread, growth, maximum burning rate and duration of the fire) [3]. As a result, detailed simulation of both the occurring physical phenomena and the layout of the compartment is needed in order to obtain reliable numerical results [4, 5, 6].

A variety of numerical tools have been developed to enable the prediction of fire growth in a compartment. The two dominant approaches are the “zone” and “field” models; the latter are essentially Computational Fluid Dynamics (CFD) tools. In zone models, the simulated compartment is coarsely divided into one or two zones, which interact with each other by exchanging mass and energy; for each zone, all physical parameters, i.e. gas temperature and species concentrations are assumed to be uniform. In CFD tools, the computational domain is divided in a fine three-dimensional mesh comprising a large number of control volumes; the fundamental equations, describing mass, momentum and energy transfer phenomena, are numerically solved for each control volume. As expected, CFD results are significantly more accurate than the respective zone model predictions [7]. In general, CFD tools have proved to be successful in a variety of fire safety problems and their role in fire research is steadily increasing as they become progressively robust and sophisticated and validation studies render them more reliable [8]. In this context, CFD codes are increasingly used to fulfil the

need for advanced design tools, capable of demonstrating compliance with performance-based fire safety regulations.

2.1 CFD Modelling of Gypsum Plasterboard Wall Assemblies Exposed to Fire

The characteristics of fire growth and spreading in a compartment fire strongly depend on the thermo-physical properties of the utilized construction materials [4, 9]. When exposed to a fire environment, the thermo-physical properties of the most commonly used construction materials vary significantly with temperature. As a result, the incorporation of temperature-dependent thermo-physical properties in relevant numerical simulations is required in order to improve the accuracy of the obtained predictions.

GP wall assemblies are utilized in a large variety of buildings. When a GP is exposed to a high temperature environment, the water molecules, initially bound in the crystal lattice of gypsum, are released; the good fire protection characteristics of GP wall assemblies are mainly owed to this, highly endothermic, GD process. GD results in two important macroscopic effects: (a) significant variation of the thermo-physical properties (e.g. density, thermal conductivity, specific heat) of the GP with increasing temperature and (b) release of modest quantities of water vapour which, by means of mass diffusion, are transported through the GP [10, 11]; however, neither of these important phenomena is taken into account in currently available CFD modelling studies of GP wall assemblies.

There is a lack of consensus regarding the appropriate methodology of effectively describing the temperature-dependent thermo-physical properties of GP [12]. The temperature-dependent physical properties of GP wall assemblies exposed to fire are commonly taken into account in the frame of one- [13] or two-dimensional heat transfer simulations; however, no relevant CFD modelling studies are available in the open literature. The release of water vapour in the fire compartment is known to significantly affect the thermal behaviour of GP wall assemblies [11]; however, water vapour mass diffusion phenomena are scarcely addressed in numerical simulations. Until now, the effects of water vapour release have been addressed in a few one-dimensional heat- and mass-transfer [2, 11, 14] simulations; there are no CFD studies available that take into account this phenomenon.

Available CFD studies focusing on simulations of full-scale GP wall assemblies exposed to fire [6, 15, 16] employ constant thermo-physical properties for gypsum, thus neglecting the physical phenomena associated with the GD process. In fact, in a recent CFD study of natural fires in an ISO 9705 room [17], it is concluded that the observed discrepancies between the obtained predictions and available experimental data are mainly attributed to the insufficient modelling of GP properties. Aiming to bridge this gap, the current study focuses on evaluating the impact of a dedicated GD model in full-scale CFD simulations of GP wall assemblies in multi-compartment buildings; the macro-scale effects of both temperature-dependent thermo-physical properties and water vapour mass diffusion phenomena are investigated.

3 NUMERICAL SIMULATION METHODOLOGY

The CFD code employed in this study is the Fire Dynamics Simulator (FDS), version 5.5.3, which has been developed by the National Institute of Standards and Technology (NIST); FDS is a CFD tool capable of simulating a large variety of fire-safety related applications, e.g. fundamental studies of fire dynamics and combustion, fire protection engineering, fire investigation, fire scene reconstruction. The Navier-Stokes equations are solved utilizing an explicit predictor-corrector scheme, second order accurate in space and time. The numerical time-step is continuously adjusted in order to satisfy the Courant-Friedrichs-Lewy (CFL) criterion; a three-dimensional, Cartesian grid is used. Turbulence is described using the Large Eddy Simulation (LES) modelling approach, which, in the context of compartment fire simulation, is suggested to provide a good balance between computational cost and numerical accuracy when compared to alternative turbulence modelling approaches (e.g. two-equation models, DNS). The subgrid-scale turbulence is simulated using a Smagorinsky constant value of 0.2.

Simulation of gas-phase combustion phenomena is accomplished by employing the conserved scalar approach (mixture fraction model), which inherently assumes that combustion is mixing-controlled (infinitely fast chemical reactions). The mixture fraction is decomposed into three components to account for local flame extinction and production or destruction of CO. Mass fractions of all the major reactants and products are derived from the mixture fraction by means of state relationships. Thermal radiation is simulated by solving the radiation transport equation, employing the finite volume method. Conjugate heat transfer in solid bodies immersed in the fluid domain is simulated by utilizing a one-dimensional heat transfer solver across each solid body; a dedicated numerical mesh, independent of the three-dimensional fluid flow mesh, is utilized in this case. Solid state pyrolysis phenomena are described utilizing the Arrhenius formulation [18]. CFD predictions of convective and radiative heat flux on the surfaces of the solid bodies are used as boundary conditions for the solid heat transfer simulations. Multi-layered wall assemblies can be simulated by utilizing detailed thermo-physical properties (e.g. density, thermal conductivity, specific heat) for each material. The FDS code has been extensively validated in a large variety of single- [3, 4, 19] and multi-compartment [6, 20] fire conditions.

3.1 Description of the Simulated Building

A two-storey residential building, located in Northern Greece, is used to perform the multi-compartment fire simulations; the building serves as a demonstration platform for investigating the energy performance of innovative construction materials and energy technologies (Figure 1, left).

Figure 1. External photograph (left) and general computational grid (right) of the simulated building.

The two-storey building, with a total area of 152 m^2, follows a typical residential arrangement plan; the living room, the kitchen and an office room can be found on the ground floor (Figure 2, right), whereas two bedrooms are located on the first floor. The building employs a load-bearing structural steel frame, whereas GP wall assemblies are used for internal partitions and external cladding. GP are installed in multi-layered wall assemblies, combined with other construction materials, in accordance to legal requirements regarding structural behaviour, fire-resistance, thermal and sound insulation.

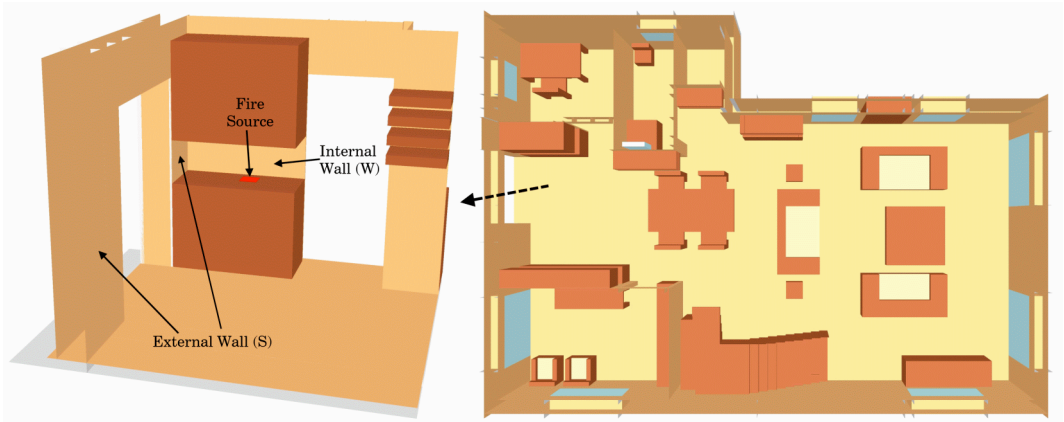

Figure 2. Top section of the ground floor of the simulated building (right) and detail of the kitchen area (left).

The layout of the multi-layered internal and external GP wall assemblies, as well as the respective thickness of each layer, are shown in Figure 3. The internal wall assembly (Figure 3, left) exhibits a symmetrical arrangement, whereas the external wall assembly (Figure 3, right) consists of two "parts" (interior and exterior), divided by a closed air cavity; the latter is used to provide space for the structural steel frame, as well as service (e.g. plumbing, electrical) networks. The floors and ceilings are constructed using multiple layers of ceramic tiles, GP and EPS insulation. All windows exhibit energy efficient double pane low-e glazing installed in insulated aluminium frames.

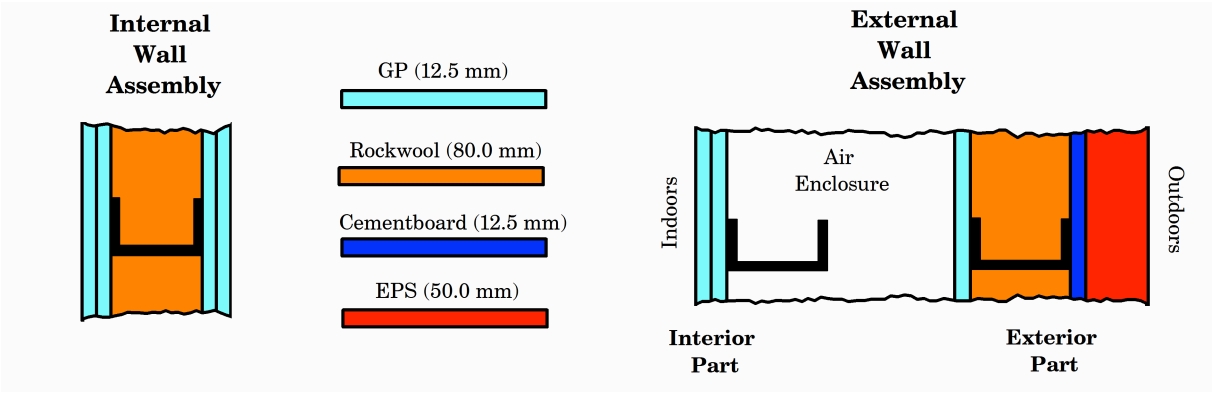

Figure 3. Cross-sections of the internal (left) and external (right) GP wall assemblies.

3.2 Computational Domain and Numerical Grid

The simulated building is considered to be completely furnished, according to a typical residential arrangement; the majority of the furniture (e.g. cupboards, benches, tables, chairs) is assumed to be made from timber. The simulated building geometry is created using the dimensions of the actual building based on architectural drawings. The computational domain used in the simulations extends approximately 1.0 m outwards from the external walls and the roof in order to take into account both ambient air entrainment and outdoors conjugate heat transfer phenomena (Figure 1, right). Overall, the computational domain dimensions are 12.8 m, 11.2 m and 8.0 m, in the x-, y- and z- directions, respectively.

A grid size of 50 mm is used in the main fire compartment (kitchen), satisfying the $D^*/\delta x$ ratio criterion ($10 < D^*/\delta x = 13.3$) that is suggested in several numerical studies [4, 21]; for the rest of the simulated building, where no flaming conditions are observed, a coarser grid size (100 mm) is utilized. Overall, the numerical grid used in the simulations consists of 967,625 cubic cells; the entire computational domain is divided in 15 numerical meshes, thus allowing the utilization of the "parallel" version of the FDS code. The independent numerical mesh used for the one-dimensional heat transfer simulations across the solid bodies consists of 42, 13 and 51 nodes, corresponding to the internal wall assembly (exhibiting a thickness of 130 mm) and the interior (25 mm) and exterior (155 mm) parts of the external wall assembly, respectively (c.f. Figure 3). The air cavity (182.5 mm), formed between the interior and the exterior part of the external wall assembly (Figure 3, right), is simulated using the fluid domain computational mesh, thus allowing accurate description of the occurring natural convection phenomena.

Since the present study focuses on the effects of GD on realistic fire conditions, a well-ventilated fire scenario is employed, aiming to minimize the effects of insufficient oxygen concentration. In this frame, the two leafs of the large French door, located in the southern side of the kitchen, are considered to be fully open for the entire duration of the simulation (Figure 2, left). As a result, given that the computational domain extends 1.0 m from the outer wall surfaces of the building, "fresh" ambient (20^oC) air is naturally entrained in the kitchen, which constitutes the main fire compartment.

3.3 Initial and Boundary Conditions

One of the most challenging aspects of performing CFD simulations of full-scale compartment fires is the appropriate implementation of the Heat Release Rate (HRR) of the fire. The temporal evolution of the HRR in full-scale compartment fires cannot be estimated using a strictly theoretical analysis; in fact, a multitude of available experimental studies focus on determining relevant semi-empirical correlations. As a result, the most commonly used approach in CFD simulations is to a priori prescribe the HRR profile of the simulated fire load by performing relevant measurements or utilizing information found in the literature [7, 22]. However, more accurate results are expected to be obtained when the related physical and chemical phenomena, such as ignition, pyrolysis, flame spread and extinction, are simulated in more detail, thus allowing a "dynamic" determination of the HRR variation with time. In a recent fire scene reconstruction studies [23], the "dynamic" HRR approach has been utilized in conjunction with the FDS code; CFD predictions have been found to be in good agreement with full-scale experimental data. In the present study, a combination of the two modelling approaches is used; a "prescribed" HRR time variation profile is employed to simulate the fire source (cooking oil pan), whereas a detailed simulation of the occurring ignition, pyrolysis, flame spread and extinction phenomena is performed to describe combustion of the main fire load (i.e. wooden furniture).

Uncontrollable fires are associated with a large range of hazards to human life, property and the environment. Amongst the large variety of fire incidents, fires in buildings are the most frequently encountered [8]; among them, the vast majority of fire-related fatalities occur in residential buildings. In general, the most prominent area of fire initiation in residential building fires is the kitchen [24]; cooking equipment is the primary cause of reported residential fires and fire-related injuries [25]. A cooking vegetable oil fire is selected as a "prescribed" fire source, aiming to simulate a typical cooking equipment fire scenario. The utilized HRR time variation profile is taken from a comprehensive report presenting oxygen calorimeter measurements of fires related to kitchen equipment and cooking vegetable oils [26], whereas the peak value of the HRR is selected according to measurements performed by NIST in a 10" pot filled with corn oil [24]; the temporal profile of the "prescribed" fire source is considered active for 557 s, exhibiting a peak HRR value of 400 kW (c.f. Figure 6). The simulated fire source is represented by a 0.2 m x 0.2 m "patch", located on the upper surface of the wooden kitchen bench (c.f. Figure 2, left).

At the beginning of the numerical simulation (t = 0 s), the entire computational domain (both indoors and outdoors) is assumed to be still (zero velocity), exhibiting a temperature of 20^{o}C. The selected total simulation time is equal to 10 min; during the simulation, the computational time-step, dynamically adjusted to satisfy the CFL criterion, varied between 4 ms and 46 ms.

3.4 Modelling of Gypsum Dehydration Phenomena

A typical GP consists essentially of a gypsum layer sandwiched between two heavy paper sheets. The crystal lattice of raw gypsum ($CaSO_4 \cdot 2H_2O$) contains approximately 21% by weight chemically bound water. When exposed to an increasing temperature environment, calcium sulphate di-hydrate ($CaSO_4 \cdot 2H_2O$) undergoes two endothermic decomposition

reactions during which the chemically bound water dissociates from the crystal lattice and evaporates. This process, known as "gypsum dehydration" (or "calcination"), occurs in the temperature region between 80°C and 250°C [27]; the advanced fire resistance characteristics of GP are owed to this effect. Gypsum chemical decomposition (dissociation of the chemically bound water) occurs in two stages [28]. In the first stage (Equation 1), calcium sulphate di-hydrate ($CaSO_4 \cdot 2H_2O$) loses 75% of its water, thus forming calcium sulphate hemi-hydrate ($CaSO_4 \cdot ½H_2O$). If gypsum is further heated, a second reaction occurs (Equation 2), where the calcium sulphate hemi-hydrate loses the remaining water to form calcium sulphate anhydrite ($CaSO_4$). Both reactions are endothermic, requiring large amounts of energy to be completed; as a result, heat transfer through a GP is practically impeded until the GD process is complete. The final products of the GD process are calcium sulphate anhydrite and water vapour; the latter is transferred through the pore network and is finally released through the GP surface.

$$CaSO_4 \cdot 2H_2O_{(s)} \rightarrow CaSO_4 \cdot {}^{1}/_{2}H_2O_{(s)} + {}^{3}/_{2}H_2O_{(g)} \quad (1)$$

$$CaSO_4 \cdot {}^{1}/_{2}H_2O_{(s)} \rightarrow CaSO_{4\,(s)} + {}^{1}/_{2}H_2O_{(g)} \quad (2)$$

In the open literature, there are no CFD studies of full-scale buildings equipped with GP wall assemblies that simulate the effects of GD, in terms of either temperature-dependent physical properties or water vapour release. Motivated by the need to quantitatively simulate the water vapour release due to GD, an innovative modelling approach based on solid reaction kinetics has been developed [29]. In the developed Gypsum Dehydration Model (GDM), the effects of GD reactions on the thermal behaviour of the GP are implemented by using a two-step solid reaction kinetics scheme, which allows the quantitative calculation of the water vapour release during the GD process. The respective reaction rates are estimated utilizing the standard first-order Arrhenius equation formulation (Equation 3).

$$\frac{\mathrm{d}Y_{s,i}}{\mathrm{d}t} = -A_i Y_{s,i}^{n} \exp\left(-\frac{E_i}{RT}\right) \quad (3)$$

The required Arrhenius parameters for each of the two GD reactions (Equations 1 and 2), are estimated by means of Differential Scanning Calorimetry (DSC) tests that have been performed using commercially available 12.5 mm GP (Type A). The thermo-chemical behaviour of gypsum is significantly affected by the heating rate [9, 10]; a relatively high heating rate value (60 K/min) was used, aiming to simulate the vigorous thermal environment encountered by GP exposed to a natural fire. As expected, the total measured GP mass loss (16.20%) is lower than the theoretical concentration of chemically-bound water in pure gypsum (21%), thus suggesting that the estimated gypsum quantity in the commercial GP sample examined is approximately 77.14%; the remainder, corresponds to various additives. Data obtained by the DSC measurements have been utilized to estimate the Arrhenius

parameters corresponding to each dehydration reaction, following the methodology proposed by Lyon [30]. The calculated Arrhenius parameters for each dehydration reaction, as well as the respective solid residue and water vapour mass yields, are presented in Table 1.

Model Parameter	Reaction 1	Reaction 2	Units
Initial Solid Component	$CaSO_4 \cdot 2H_2O$	$CaSO_4 \cdot {}^1/_2H_2O$	-
Solid Residue	$CaSO_4 \cdot {}^1/_2H_2O$	$CaSO_4$	-
v_{res}	87.85 %	95.20 %	-
v_{H2O}	12.15 %	4.80 %	-
A	1.16407×10^{17}	2.95661×10^{7}	s^{-1}
E	148636.15	78628.42	kJ/kmol
n	1	1	-
Endothermic Heat	329.79	109.93	kJ/kg

Table 1. Kinetic parameters used for the gypsum dehydration solid reaction kinetics model.

3.5 Modelling of Wood Pyrolysis and Combustion

The simulated building is assumed to be primarily equipped with wooden furniture, which corresponds to the main fire load. When wood is heated, solid phase pyrolysis reactions are initiated; the produced combustible gases are released to the adjacent environment where, when proper thermal and mixing criteria are met, they are ignited, thus resulting in the development of flaming conditions. Pyrolysis decomposition reactions are strongly dependent on temperature; the respective reaction rates are typically described utilizing an Arrhenius equation formulation (Equation 3). Proper selection of reliable values for the pyrolysis rate coefficients (A_i, n, E_i) of solid combustible materials poses a significant challenge, since the respective, experimentally obtained, values may exhibit differences of several orders of magnitude. A single-step Arrhenius reaction is used in this study to model the thermal decomposition (pyrolysis) reactions of wood (oak). The utilized kinetic and thermal parameters used in the simulations are taken from the literature [31]; the respective values are presented in Table 2. It is assumed that 23.1% of the combustible wood is converted to char [31]. The (fixed) mass yield of carbon monoxide (CO) is assumed to be 0.004 kg CO/kg wood, according to relevant suggestions found in the literature [32]. The combustible gases produced by wood pyrolysis are described by the collective chemical species $C_6H_{10}O_5$; a simplified two-step reaction model is used to simulate gaseous combustion.

Parameter	Symbol	Value	Units
Pre-exponential factor	A	5.49×10^{12}	s^{-1}
Activation energy	E	1.7×10^{5}	kJ/kmol
Reaction order	n	3.56	-
Heat of combustion	ΔH_C	15	MJ/kg

Table 2. Kinetic parameters utilized to describe wood pyrolysis phenomena.

3.5 Parametric Study

Currently available CFD simulations of GP wall assemblies describe the thermal behaviour of gypsum by employing constant thermo-physical properties [6, 17, 16]; as a result, GD phenomena are not taken into account. In this work, a parametric study is performed, aiming to investigate the effect of GD on the predictions of CFD simulations focusing on a full-scale building exposed to fire. Two different alternative approaches are used to describe the thermo-chemical behaviour of GP wall assemblies. In the first modelling approach (NO), which serves as a benchmark, a set of constant thermo-physical properties is used, pertaining to the "conventional" CFD simulation methodology, where no GD phenomena are taken into account. The employed values correspond to the thermo-physical properties of $CaSO_4 \cdot 2H_2O$ at room temperature; the utilized values are similar to the respective values used in relevant CFD simulations [6, 17, 16]. The second modelling approach (GDM) utilizes a two-step Arrhenius equation formulation to describe the solid reaction kinetics of the GD process. The GDM allows quantification of GD thermal effects and water vapour production.

4 RESULTS AND DISCUSSION

The main features of the fire-induced flow-field developing inside the simulated building are depicted in Figure 4, where streak lines for fluid elements originating from the fire source, at three characteristic time instants, are presented. A thermally-induced upward flow is quickly established in the kitchen above the region of the fire source; the developing ceiling jet soon expands laterally to the adjacent rooms and eventually, through the slanting roof of the living room, to the upper floor. Two large counter-rotating vortices are formed when the developing hot layer reaches the upper floor. The highest gas-phase velocity values are observed near the fire source, where the large temperature gradients result in a strong buoyant upward flow. A typical stratified fire-induced flow-field is eventually developed in both floors; "fresh" ambient air is entrained through the lower part of the open door, located at the southern wall of the kitchen.

Predictions of the maximum heat release rate iso-surface, corresponding to the location and shape of the simulated flame "envelope", are also depicted in Figure 4. It is evident that the fire envelope, which initially extends just above the simulated fire source, quickly engulfs the wooden cupboard located above the kitchen bench (2 min) and it gradually moves upwards until it finally reaches the upper side of the cupboard (5 min). The "peak" of the fire envelope size is observed approximately 5 min after the fire initiation; soon after, the fire envelope begins to recede, until it becomes virtually extinct (8 min). Overall, the developing fire cannot be sustained when the "prescribed" fire source wears out. This can be attributed to a variety of reasons, such as the high radiative losses to the environment through the open French door, the large indoor openings that facilitate internal flow circulation and thermal energy dissipation, the large volume of the entire building which serves as a "thermal fly-wheel", absence of materials that would allow fast propagation of the flame (e.g. paper, fabric). As a

result, no flashover is observed, despite the ample supply of fresh ambient air (over-ventilated fire conditions).

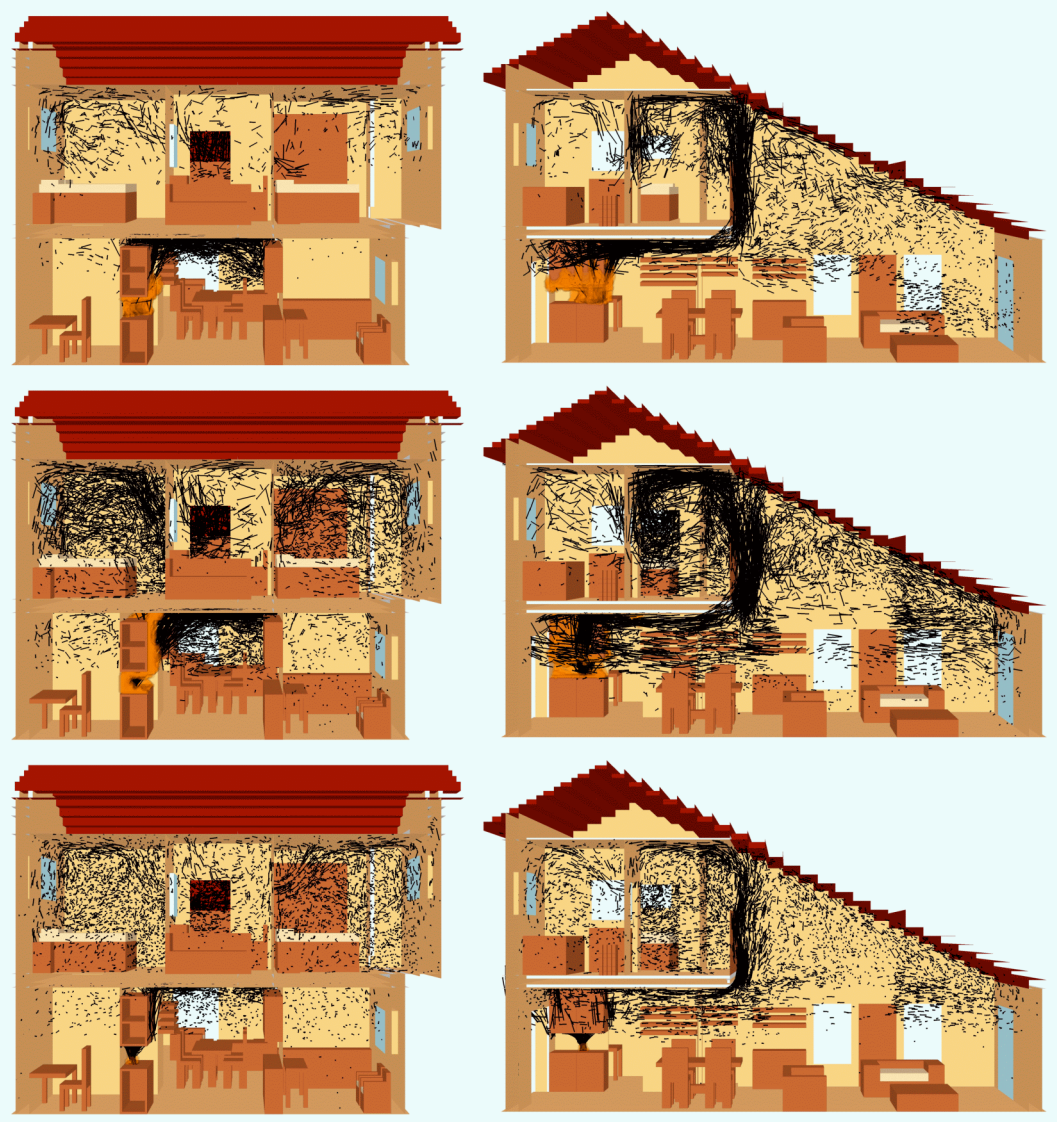

Figure 4. Predictions of flame envelope and streak lines for fluid elements originating from the fire source, 2 min (top), 5 min (middle) and 8 min (bottom) after fire initiation (GDM).

Predictions of the gas temperature distribution inside the building, for three characteristic time instants, are depicted in Figure 5. As expected, the maximum temperatures are observed in the region just above the fire source, where the main fire plume is located. The most prominent feature of the developing thermal field is the expanding hot layer, which is quickly established under the ceiling of the kitchen and gradually moves towards the adjacent rooms. The characteristics of the developing stratified thermal field are evident on the ground floor; the buoyant combustion products move upwards, thus forming a hot gas layer, whereas colder air is drawn in the lower part; thermal stratification, although less distinct, is also observed in the upper floor. Fresh air entrainment through the open French door is evident in the lower part of the kitchen room.

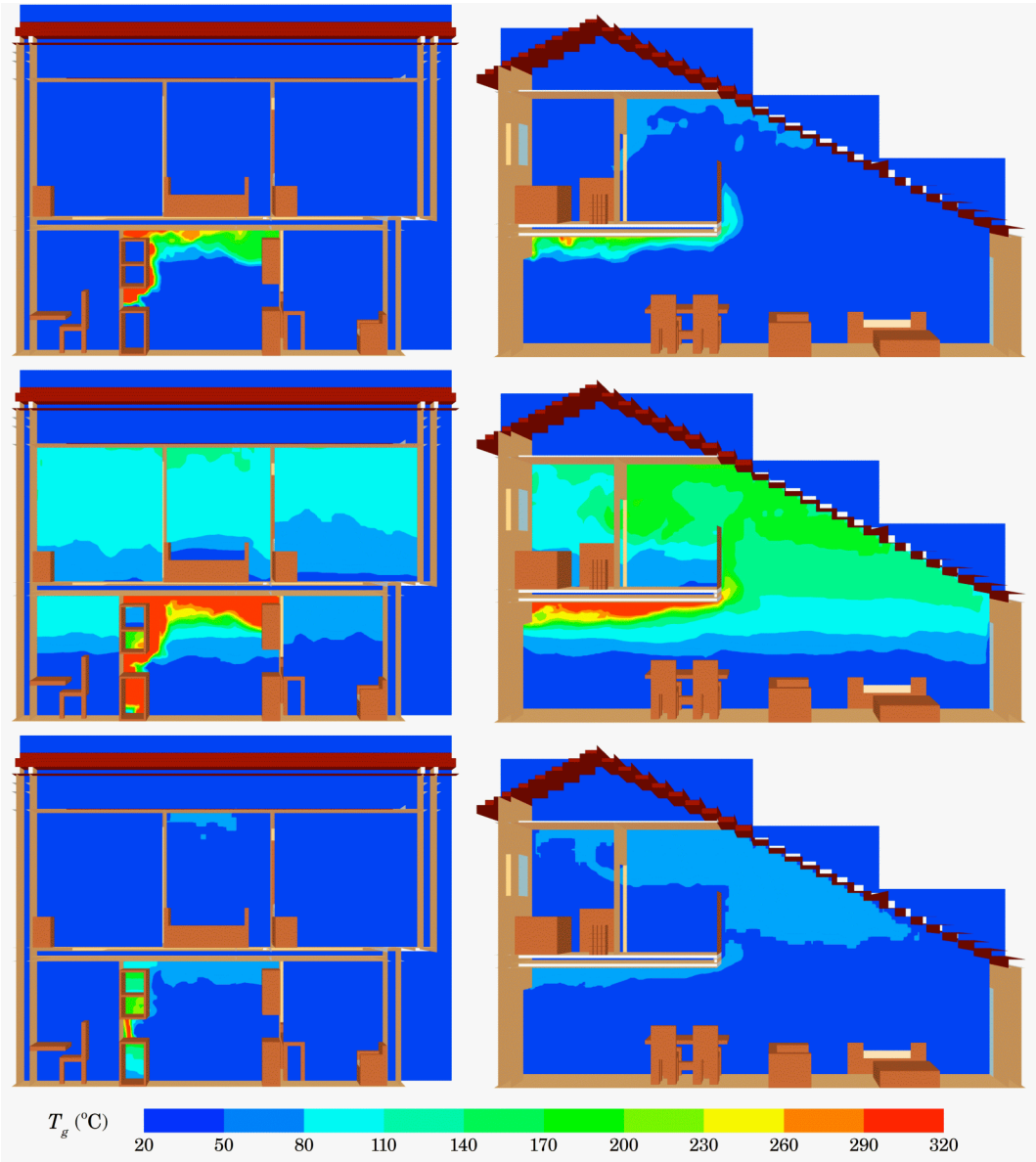

Figure 5. Predictions of gas phase temperature, 2 min (top), 5 min (middle) and 8 min (bottom) after fire initiation (GDM).

4.1 Thermal Effects of Gypsum Dehydration

In order to investigate the various characteristic stages of the developing fire, predictions of the temporal evolution of the overall HRR, along with the "prescribed" HRR profile used to simulate the fire source are depicted in Figure 6, for both the examined test cases. Combustion of the "actual" fire load (wooden furniture) initiates approximately 2 min after the start of the simulation, when significant heat is released in the "prescribed" fire source. The predicted overall HRR quickly increases, reaching a "peak" approximately 4.5 min after the fire initiation; when the "prescribed" fire source is practically quenched (5 min), wood pyrolysis reactions cannot be sustained and the overall HRR predictions exhibit a rapid decrease. As expected, when GD phenomena are not taken into account (NO), higher peak HRR values are predicted; predictions of the net thermal energy release using the NO model result in an approximately 13% higher value than the respective predictions using the GDM, thus suggesting that GD phenomena have a clear impact on the overall fire heat release.

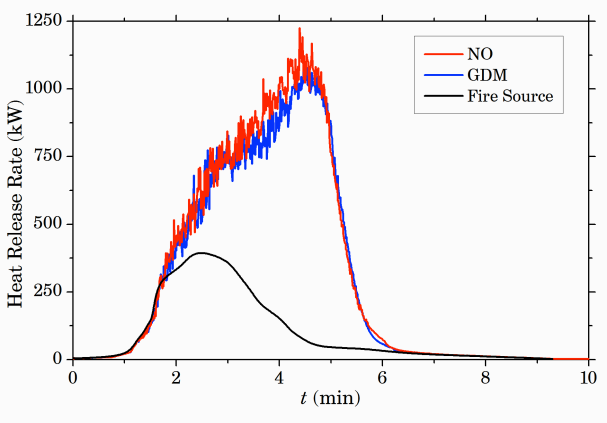

Figure 6. Temporal evolution of the "prescribed" fire source and the predicted overall heat release rate.

The effect of modelling the GD process is also evident in Figure 7, where predictions of the temporal evolution of the gas temperature are depicted for two characteristic positions; the first, located 0.2 m above the simulated fire source, corresponds to the main "fire region"; the second, located at the centre of the kitchen room, 0.1 m under the ceiling, is representative of the prevailing conditions in the expanding "hot layer". The sudden drop in the predicted gas temperatures observed in all cases, approximately 5 min after fire initiation, follows closely the behaviour of the HRR temporal profile (Figure 6). Since temperatures in the fire region are mainly determined by the imposed "prescribed" HRR, the observed discrepancies among the temperature predictions of the two investigated test cases are minimal. However, gas temperatures in the developing hot layer exhibit modest differences; when constant physical properties are used (NO), predicted gas temperatures are generally higher than the respective values obtained by simulating the GD process (GDM). In the latter case (GDM), the thermal energy needed for the highly endothermic gypsum dehydration reactions is essentially removed from the gaseous environment, thus resulting in lower average gas temperatures.

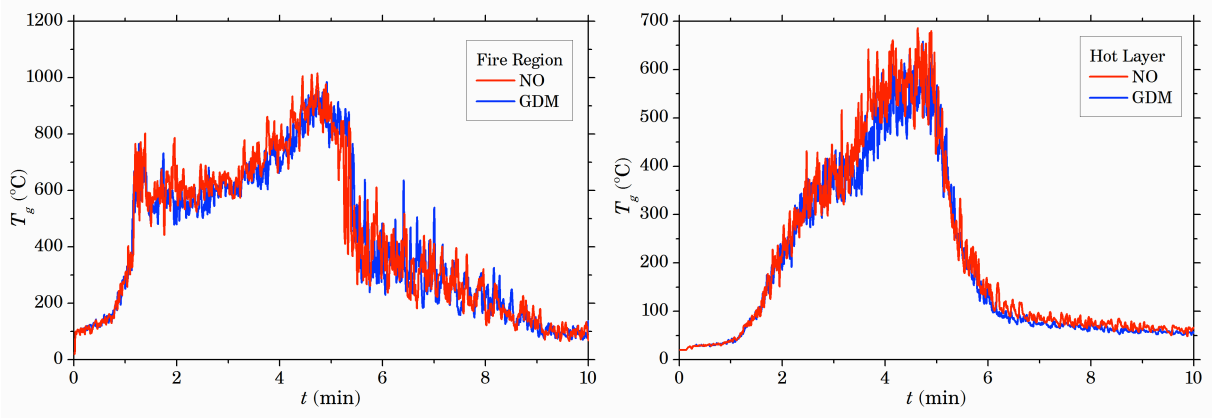

Figure 7. Temporal evolution of gas temperature predictions in the fire region (left) and the hot layer (right).

CFD simulations may be utilized to assess the fire resistance characteristics of building elements when exposed to realistic fire conditions. In general, the non load-bearing building elements that are used for "compartmentation" purposes are expected to prevent fire spread or ignition beyond the exposed surface during a fire incident. According to the Eurocode standards [33], the "separating function" of non load-bearing elements is ensured when the

"integrity" (E) and "insulation" (I) fire resistance criteria are fulfilled; the latter is considered to be satisfied when the average temperature rise over the unexposed surface of the building element is limited to 140 K. The "insulation" criterion was used to assess the fire resistance of the GP wall assemblies; in order to fulfil this criterion, the temperature of the unexposed side should not exceed 160°C (20°C being the ambient temperature).

Surface temperature predictions at the exposed and unexposed side of two characteristic walls, located adjacent to the fire source, are depicted in Figure 8; the first position corresponds to the centre of the western internal wall, whereas the second position is located at the western part of the interior assembly of the southern external wall (c.f. Figure 2, left). The depicted predictions correspond to a height of 1.4 m above the floor. Predictions of the exposed surface temperatures in both cases are qualitatively and quantitatively similar; the initial rapid increase of the predicted temperatures is followed by a more gradual decrease until the end of the simulation time. The maximum temperature values achieved (approximately 700°C), may lead to the emergence of cracking phenomena; such effects are neglected in the current study. When the GD phenomena are not taken into account (NO), wall surface temperature predictions are consistently higher, during both the heating and the cooling phase. The unexposed side of the internal wall assembly, which consists of two GP pairs, separated by an 80 mm insulation layer (c.f. Figure 3, left) exhibits a nearly negligible temperature rise; in fact, the predicted temperatures lie very close to the initial ambient temperature (20°C). However, temperature predictions for the unexposed side of the interior assembly of the external wall, comprising only two GP joined together (c.f. Figure 3, right), are gradually increasing, without, however, reaching the critical "failure" value of 160°C. Once more, the effect of GD modelling is evident; the final (10 min) temperature of the external wall's unexposed surface using the NO model (134°C) is approximately twice the respective value utilizing the GDM (61°C).

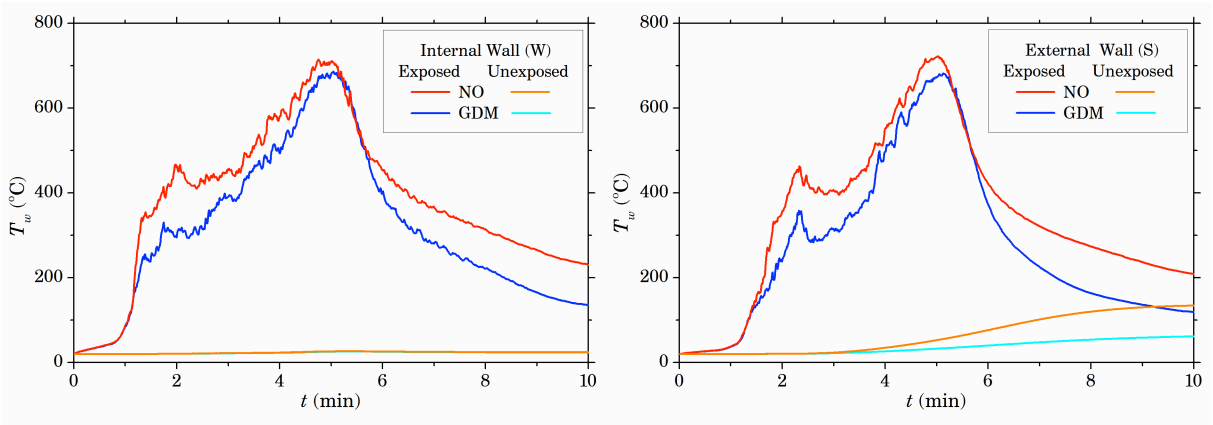

Figure 8. Temporal evolution of exposed and unexposed surface temperature predictions for the internal (W) wall (left) and the interior assembly of the external (S) wall (right).

Aiming to further illustrate the impact of gypsum dehydration on the temperature that a GP wall assembly may achieve when exposed to fire, predictions of wall surface temperatures in the main fire compartment, 5 min after fire initiation, are depicted in Figure 9, for both test cases. As expected, peak temperatures are observed in the walls that are directly adjacent to

the fire source. A vertically stratified wall temperature distribution is observed far from the fire envelope. Intense heating of the wooden cupboard just above the fire source results in increasing temperatures, which, in turn, intensify wood pyrolysis reactions. It is evident that when GD phenomena are neglected (NO), predicted wall surface temperatures are, on average, higher.

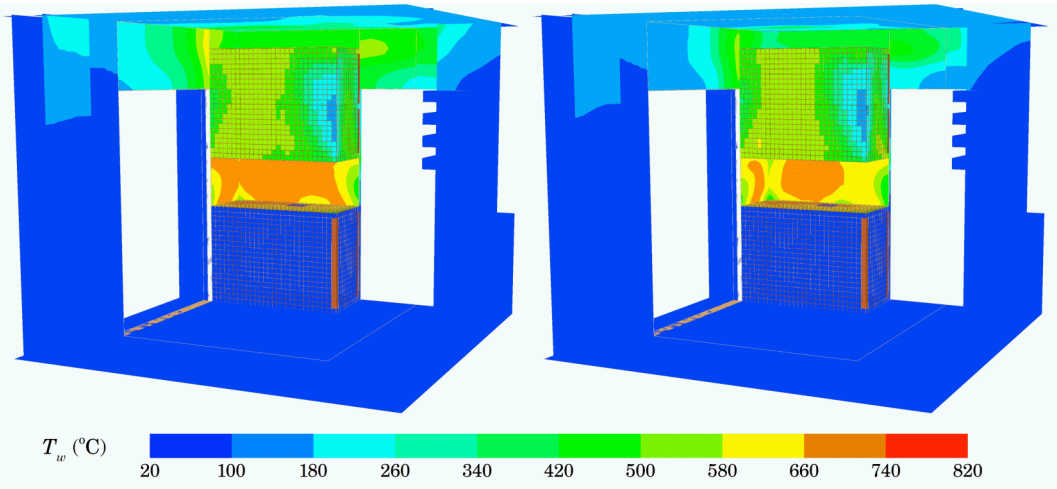

Figure 9. Predictions of kitchen wall surface temperatures, 5 min after fire initiation, using the NO (left) and GDM (right) models.

4.2 Effects of Water Vapour Release due to Gypsum Dehydration

The GDM used in this study, allows, for the first time in the frame of CFD simulations, quantification of the water vapour release rate through the GP wall assemblies due to the gypsum dehydration process [29]. Predictions of the temporal evolution of the water vapour mass content in the fire compartment are depicted in Figure 10; the reported values correspond to water vapour produced due to combustion, as well as due to GD. It is evident that GD phenomena result in the production of significant water vapour quantities, which may contribute up to 30% to the overall water vapour content. The favourable impact of the "additional" water vapour production is two-fold; it reduces the mean temperature of the gaseous mixture and it further decreases the overall O_2 concentration in the fire compartment.

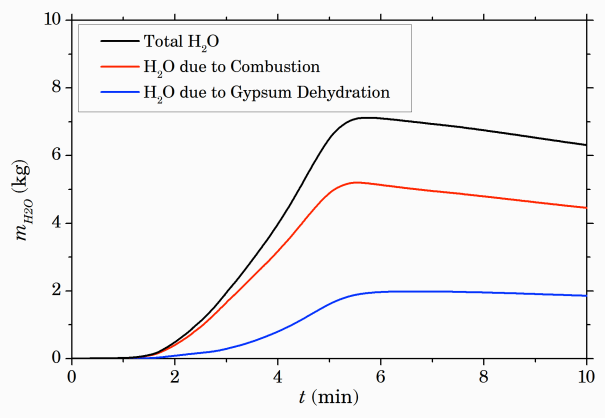

Figure 10. Temporal evolution of the overall water vapour mass in the building (GDM).

Predictions of the temporal evolution of water vapour mass flow rate through the GP wall assemblies of the main fire compartment (kitchen), for three characteristic time instances, are depicted in Figure 11. As expected, higher GD rates (and thus water vapour production rates) are observed in the walls that are adjacent to the fire source (2 min); the gradual extension of the fire envelope (5 min) initiates GD reactions also at the GP assembly of the ceiling. When the overall fire intensity is decreased (8 min), certain parts of the GP wall assemblies that still exhibit high temperatures undergo GD reactions.

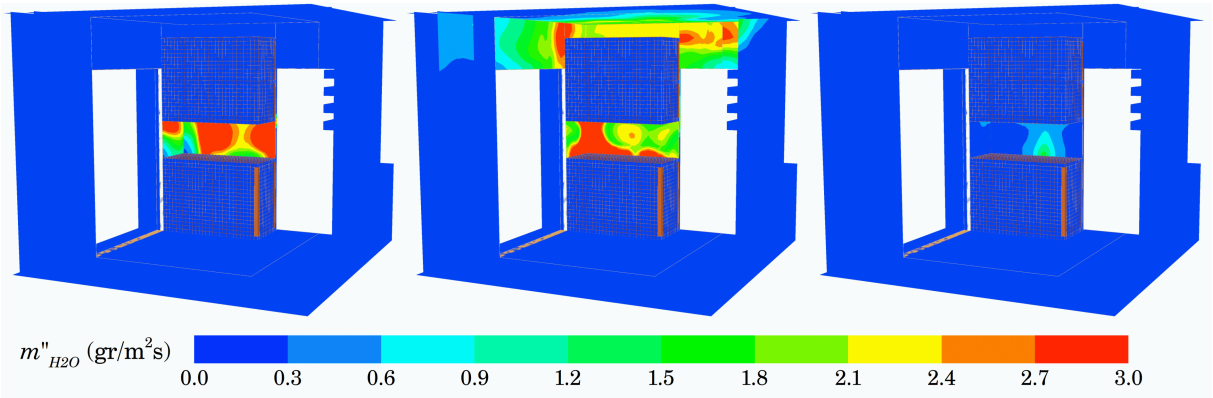

Figure 11. Predictions of gypsum dehydration induced water vapour mass flux through the kitchen wall exposed surfaces, 2 min (left), 5 min (middle) and 8 min (right) after fire initiation (GDM).

The capabilities of the developed GDM, in terms of predicting GD induced water vapour production and dispersion are illustrated in Figure 12, where predictions of the GD induced water vapour mass fraction distribution inside the simulated building are depicted. The water vapour produced in the main fire compartment (kitchen) is entrained by the developing flow-field; as a result, it is gradually transported to the adjacent rooms. Owed to the comparatively low density of the water vapour, a distinct stratified concentration field is eventually developed, when the main combustion (and flow) activity has, practically, ceased (8 min).

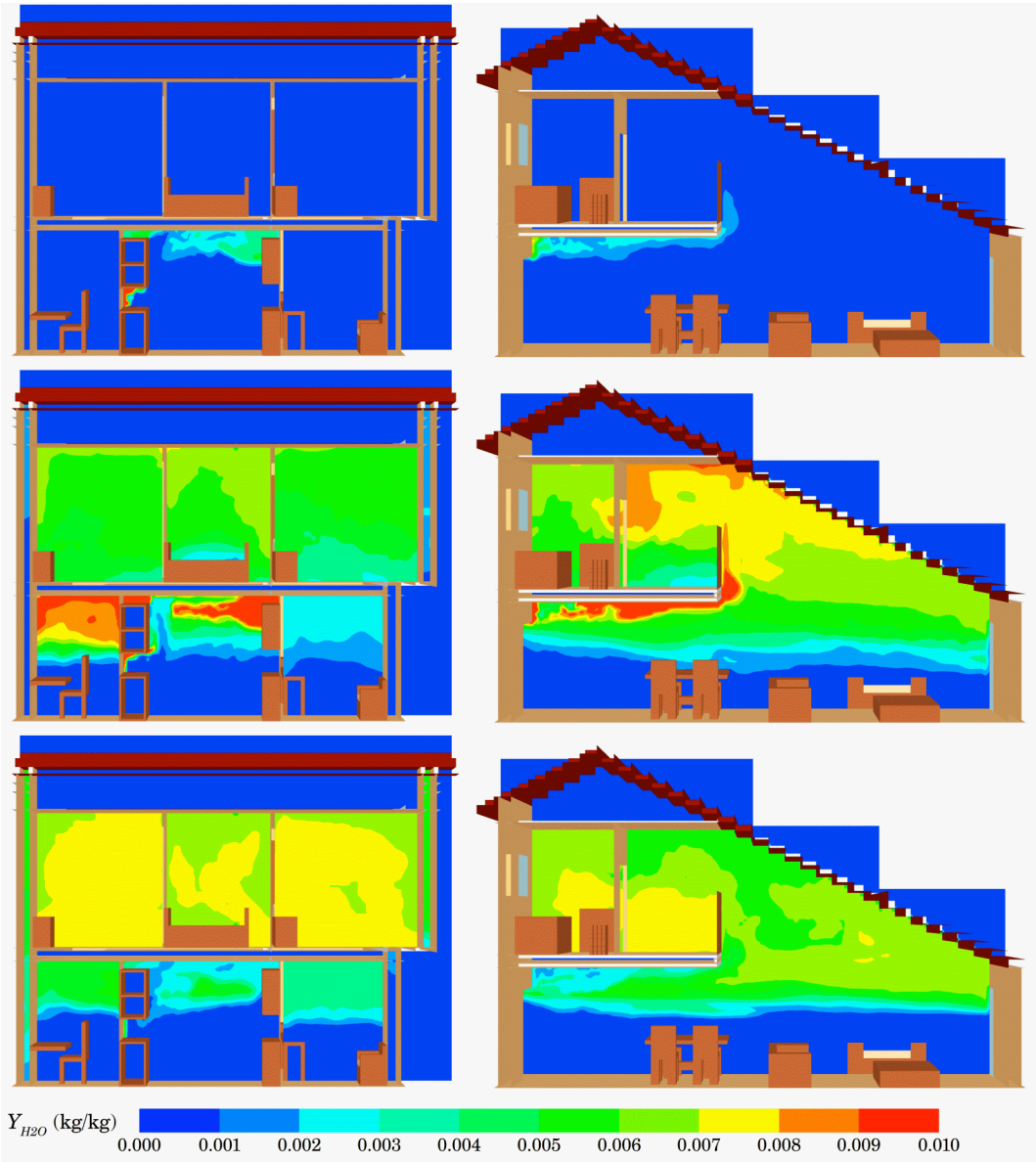

Figure 12. Predictions of gypsum dehydration induced water vapour mass fraction, 2 min (top), 5 min (middle) and 8 min (bottom) after fire initiation (GDM).

5 CONCLUSIONS

The incorporation of gypsum dehydration modelling in CFD simulations of gypsum plasterboard wall assemblies exposed to fire has been thoroughly investigated. The FDS code has been utilized to simulate a typical cooking equipment fire scenario in a full-scale two-storey residential building. The simulated building is constructed using a load-bearing steel frame combined with multi-layered gypsum plasterboard wall assemblies. The effects of gypsum dehydration and the associated water vapour release have been investigated by using a dedicated solid reaction kinetics model, which allowed, for the first time, quantification of the gypsum dehydration induced water vapour; relevant predictions of water vapour production and dispersion have been presented. It has been shown that when the highly endothermic gypsum dehydration phenomena are simulated, lower overall heat release rate,

gas and wall surface temperature values are predicted. Simulation of wall temperatures allowed the assessment of the fire resistance behaviour of the full scale building. All gypsum plasterboard wall assemblies have been shown to retain their "separating function" for the entire duration of the 10 min simulation time; however, when gypsum dehydration phenomena are taken into account, the corresponding fire resistance characteristics are noticeably improved. Overall, it has been shown that the CFD predictions are clearly affected when gypsum dehydration phenomena are incorporated in the simulation. As a result, utilization of such advanced physical models is strongly advised for simulations requiring increased accuracy, e.g. in the implementation of CFD tools for demonstrating compliance with performance-based codes.

ACKNOWLEDGMENTS

The present study has been financially supported by the E.C. in the frame of the EU-FP7 project titled "MESSIB: Multi-source Energy Storage System Integrated in Buildings" (NMP2-LA-2008-211624).

REFERENCES

1. Zalok, E. and Hadjisophocleous, G.V., Assessment of the use of Fire Dynamics Simulator in performance-based design, *Fire Technology*, **47**, 2011, pp. 1081–1100.
2. Wang, C.Y. and Ang, C.N., The effect of water movement on specific heat of gypsum plasterboard in heat transfer analysis under natural fire exposure, *Construction and Building Materials,* **18**, 2004, pp. 505-515.
3. C. H. Hwang, A. Lock, M. Bundy, E. Johnsson, G.H. Ko, Studies on fire characteristics in over- and under ventilated full-scale compartments, *Journal of Fire Sciences*, **28**, 2010, pp. 460-486.
4. Jahn, W., Rein, G., and Torero, J.L., A posteriori modelling of the growth phase of Dalmarnock Fire Test One, *Building and Environment*, **46**, 2011, pp. 1065-1073.
5. Rein, G., Torero, J.L., Jahn, W., Stern-Gottfried, J., Ryder, L.N., Desanghere, S., Lazaro, M., Mowrer, F., Coles, A., Joyeux, D., Alvear, D. , Capote, A.J., Jowrsey, A., Abecassis-Empis, C. and Reszka, P., Round-robin study of a priori modelling predictions of the Dalmarnock Fire Test One, *Fire Safety Journal*, **44**, 2009, pp. 590-602.
6. Boehmer, H., Floyd, J. and Gottuk, D.T., Fire dynamics and forensic analysis of limited ventilation compartment fires Volume 2: Modeling, Hughes Associates, Baltimore, USA, 2009.
7. Rein, G., Bar-Ilan, A. and Fernandez-Pello, C., A comparison of three models for the simulation of accidental fires, *Journal of Fire Protection Engineering*, **16**, 2006, pp. 183-209.
8. Yeoh, G.H. and Yuen, K.K., Computational Fluid Dynamics in Fire Engineering, 2009, Elsevier, Butterworth-Heinemann, Oxford.

9. Jahn, W., Rein, G. and Torero, J.L., The effect of model parameters on the simulation of fire dynamics, *Fire Safety Science*, **9**, 2008, pp. 1341-1352.
10. Kontogeorgos, D.A. and Founti, M.A., Numerical investigation of simultaneous heat and mass transfer mechanisms occurring in a gypsum board exposed to fire conditions, *Applied Thermal Engineering*, **30**, 2010, pp. 1461-1469.
11. Van der Heijden, G.H.A., Pel, L., Huinink, H.P. and Kopinga, K., Moisture transport and dehydration in heated gypsum, an NMR study, *Chemical Engineering Science*, **66**, 2011, pp. 4241-4250.
12. Hopkin, D.J., Lennon, T., El-Rimawi, J. and Silberschmidt, V.V., A numerical study of gypsum plasterboard behavior under standard and natural fire conditions, *Fire and Materials*, **36**, 2012, pp. 107-126.
13. Kontogeorgos, D., Wakili, K.G., Hugi, E. and Founti, M., Heat and moisture transfer through a steel stud gypsum board assembly exposed to fire, *Construction and Building Materials*, **26**, 2012, pp. 746-754.
14. Craft, S.T., Isgor, B., Hadjisophocleous, G. and Mehaffey, J.R., Predicting the thermal response of gypsum board subjected to a constant heat flux, *Fire and Materials*, **32**, 2008, pp. 333-355.
15. Novozhilov, V., Computational fluid dynamics modelling of compartment fires, *Progress in Energy and Combustion Science*, **27**, 2001, pp. 611-666.
16. Lopes, A.M., Vaz, G.C. and Santiago, A., Numerical predictions of the time-dependent temperature field for the 7th Cardington compartment fire test, Steel and Composite Structures, **5**, 2005, pp. 421-441.
17. Moinuddin, K.A.M., Al-Menhali, J.S., Prasannan, K. and Thomas, I.R., Rise in structural steel temperatures during ISO 9705 room fires, *Fire Safety Journal*, **46**, 2011, pp. 480-496.
18. McGrattan, K., Baum, H., Rehm, R., Mell, W., McDermott, R., Hostikka, S. and Floyd, J., Fire Dynamics Simulator (Version 5) Technical Reference Guide, Volume 1: Mathematical Model, NIST Special Publication 1018-5.
19. Yang, D., Hu, L.H., Jiang, Y.Q., Huo, R., Zhu, S. and Zhao, X.Y., Comparison of FDS predictions by different combustion models with measured data for enclosure fires, *Fire Safety Journal*, **45**, 2010, pp. 298-313.
20. Pope, N.D. and Bailey, C.G., Quantitative comparison of FDS and parametric fire curves with post-flashover compartment fire test data, *Fire Safety Journal*, **41**, 2006, pp. 99-110.
21. Lin, C.H., Ferng, Y.M. and Hsu, W.S., Investigating the effect of computational grid sizes on the predicted characteristics of thermal radiation for a fire, *Applied Thermal Engineering,* **2**, 2009, pp. 2243-2250.
22. Yuan, S. and Zhang, J., Large eddy simulation of compartment fire with solid combustible, *Fire Safety Journal*, **44**, 2009, pp. 349-362.
23. Yang, P., Tan, X. and Xin, W., Experimental study and numerical simulation for a storehouse fire accident, *Building and Environment*, **46**, 2011, pp. 1445-1459.

24. Madrzykowski, D. and Hamins, A., Residential kitchen fire suppression research needs: Workshop Proceedings, NIST Special Publication 1066, Washington, USA, 2007.
25. Ahrens, M., Hall, J., Comoletti, J., Gamache, S. and LeBeau, A., Behavioral mitigation of cooking fires through strategies based in statistical analysis, U.S. Fire Administration, Final Project Report EME-2005-CA-0343.
26. Robbins, A.P., Residential kitchen local fire protection - Experiments, BRANZ Study Report SR 225, BRANZ, Judgefors, New Zealand, 2010.
27. Paulik, F., Paulik, J. and Arnold, M., Thermal decomposition of gypsum, *Thermochimica Acta*, **200**, 1992, pp. 195-204.
28. Thomas, G., Thermal Properties of Gypsum Plasterboard at High Temperatures, *Fire and Materials*, **26**, 2002, pp. 37-45.
29. Kolaitis, D.I. and Founti, M.A., Development of a Solid Reaction Kinetics Gypsum Dehydration Model Appropriate for CFD Simulation of Gypsum Plasterboard Wall Assemblies Exposed to Fire, *Submitted to Fire Safety Journal* (2012)
30. Lyon, R.E., An integral method of nonisothermal kinetic analysis, *Thermochimica Acta*, **297**, 1997, pp. 117-124.
31. Matala, A., Estimation of solid phase reaction parameters for fire simulation, M.Sc. Thesis, Helsinki University of Technology, 2008.
32. DiNenno, P.J., Drysdale, D., Beyler, C.L., Walton, W.D., Cruster, R.L.P., Hall, J.R. and Watts, J.M., S.F.P.E. Handbook for Fire Engineering, 2002, 3rd Edition, National Fire Protection Association, USA.
33. EN 1991-1-2, Eurocode 1: Actions on structures - Part 1-2: General actions - Actions on structures exposed to fire, European Committee for Standardization, 2002.